Thin Solid Films 612 (2016) 29–35

Contents lists available at ScienceDirect

Thin Solid Films

journal homepage: www.elsevier.com/locate/tsf

Influence of Fe(Cr) miscibility on thin film grain size and stress

Xuyang Zhou, Tyler Kaub, Richard L. Martens, Gregory B. Thompson *

The University of Alabama, Department of Metallurgical & Materials Engineering, Tuscaloosa, AL, USA

ARTICLE INFO

Article history:
Received 16 September 2015
Received in revised form 5 April 2016
Accepted 16 May 2016
Available online 18 May 2016

Keywords:
Stress evolution
Thin films
Iron alloy
Chromium alloy
Atom probe tomography
Segregation

ABSTRACT

During the post coalescence portion of thin film deposition, thin film stress is related to the grain size and adatom mobility of the depositing material. Using a Fe(Cr) alloy thin film, the manipulation of the tensile stress for thick films was studied as a function of Cr solute content up to 8 at.%. Solute concentrations up to 4 at.% resulted in an approximate 50% increase in grain size that resulted in a reduction of the tensile stress to be lower than either elemental film. Upon increasing the Cr content, the grain size refined and the tensile stress of the films increased. Atom probe characterization of the grain boundaries confirmed Cr chemical partitioning which refined the grain size and altered the film's texture, both of which contributed to the change in film stress. The use of intrinsic segregation, rather than deposition processing parameters, appears to be another viable option for regulating film stress.

1. Introduction

Thin films are a vital architecture in several technologically important applications including information storage [1], optical devices [2,3], semiconductor transistor design [4,5], energy harvesting [6,7], and tribological coatings [8]. In these applications, the intrinsic thin film stress plays a fundamental role in tuning physical and mechanical properties [9–15]. By understanding stress evolution during thin film growth, and even controlling the stress state in the thin film, one can enhance the reliable performance of such thin film based devices and help improve their functional properties.

In general, researchers have focused on understanding the in situ stress evolution of thin films consisting of single element species [16–26]. It is generally accepted that initial compressive stress at the first stage of growth is a result of the atomic-scale migration into embryonic islands that form to minimize surface area-to-volumetric energies. After then a subsequent tensile stress is generated by the elastic strain created from the islands as they begin to coalesce. Once coalescence is complete, thin films with high adatom mobility, such as Cu, Ag and Co, experience a return to a compressive stress state through the adatom diffusion into grain boundaries [21,27,28]. However, elemental films with low adatom mobility, like Fe [29], Cr [29], and Al [19], usually tend to retain the coalescence-induced tensile condition with continued growth. The final thin film stress will be the competition between coalescence-induced tensile stress and adatom diffusion into the grain boundaries generating a compressive stress response.

This stress state can be influenced by several experimental parameters including deposition rate and substrate temperature which alter the adatom mobility [29,30]. For example, in the case of electrodeposited Ni, when deposited at a high growth rate, this film exhibits a tensile stress. As the growth rate decreases, a compressive stress is created through the adatom diffusion into the grain boundaries which dominate the coalescence-induced tensile stress mechanisms. Similarly, increasing the temperature is akin to decreasing the deposition rate. At an elevated temperature, this transition from tensile stress to compressive stress has been noted in elemental Fe film deposition [29].

The stress state of a thin film can also be controlled by regulating the microstructure of the film. In elemental species films, changes in grain size have been shown to directly correlate with the stress state of the film [20]. Such a change in grain size can be accomplished through the substrate temperature, deposition rate, and deposition pressure [31,32]. Unlike these prior single element films, an alloy film has the added complexity of different adatom interactions in regulating the film microstructure. These interactions could alter initial island sizes and coalescence behavior through changes in surface and grain boundary energies. For example, Fu and Thompson reported how the stress state of a Fe-Pt thin film changed based on the composition of the grain boundary [33]. In this case, the mixing of Fe, a low adatom mobility species, and Pt, a high adatom mobility species, resulted in a range of tensile to compressive stresses dependent on the composition in the grain boundaries.

In this paper, we aim to further investigate alloy behavior on film microstructure and growth stress states. Unlike the former work in Fe-Pt, where each individual species had a different stress response (tensile or compressive) [33], this paper addresses Fe-Cr alloy films where both individual species have a tensile or lower adatom mobility

* Corresponding author.
E-mail address: gthompson@eng.ua.edu (G.B. Thompson).

http://dx.doi.org/10.1016/j.tsf.2016.05.024
0040-6090/

behavior. In this study, we will be able to elucidate how mixing similar adatom mobility alloy elements alters the intrinsic tensile growth stresses. Moreover, Fe-Cr exhibits a miscibility gap which would indicate a strong preference for chemical partitioning to the interfaces which could also influence the segregation of specific species to the grain boundaries and alter the aforementioned interface/grain boundary energies.

2. Experimental

Elemental and alloyed nanocrystalline thin films of Fe, Cr and $Fe_{1-x}Cr_x$ were sputter deposited from 99.95 at.% pure Fe and Cr targets in an AJA ATC-1500 stainless steel magnetron-sputtering system. The films were grown to an approximate thickness of 300 nm on to 300 μm thick Si [001] substrates, with a native surface oxide, at ambient temperature. The sputtering rates were 0.11 nm/s for Fe, 0.14 nm/s for Cr and 0.11–0.14 nm/s for the alloys dependent on composition. The base pressure prior to sputtering was $<6 \times 10^{-6}$ Pa whereupon ultra-high-purity argon was introduced as the working gas at a flow rate of 10 standard cubic centimeters per minutes to a pressure of 0.27 Pa.

The in situ stress state was measured through a K-Space Multi-beam Optic Sensor attached onto the sputter chamber [34]. By reflecting a series of laser spots from the substrate to a charge-coupled detector, the relative position of the spots changes as the substrate bends in response to the growth stresses. Using the Stoney equation, given below, the stress within the film was measured and calculated.

$$\sigma_f = \frac{E_s}{6(1-\nu_s)}\frac{t_s^2}{t_f}\left(\frac{1}{R}-\frac{1}{R_0}\right) \quad (1)$$

where σ_f is the average films stress, ν_s and E_s are the Poisson ratio and the Young's modulus of the substrate respectively, t_f is the film thickness, and $1/R_0$ and $1/R$ are measured curvatures of the films before and during the deposition.

Post deposition, the compositions of the alloy thin films were verified from the co-sputtering calculations using Energy Dispersive X-ray Spectroscopy in a TESCAN LYRA dual electron-focus ion beam (FIB) microscope operated at 20 keV. X-Ray Diffraction (XRD) was performed for phase identification via a Philips diffractometer with Cu K_α radiation as the source operated at 45 kV and 40 mA. XRD pole figures for orientation analysis were also collected using a Bruker D8 GADDS diffractometer.

Transmission electron microscopy (TEM) was performed in an FEI Tecnai SupertwinF20 microscope. The TEM plan-view foils, prepared by cutting, dimpling and ion-milling a 3 mm disc, were also used to confirm phase as well as grain sizes and grain boundary character types using the NanoMEGAS Precession Electron Diffraction (PED) platform. The details of how the NanoMEGAS platform works can be found in reference [35]. The PED scanning was operated with a 0.2° procession angle and a scanning step size of 4 nm, in the same size of region of interest (ROI), which was 1.5 μm × 1.5 μm. After scanning, the data was converted for analysis using TSL OIM Analysis 5 software. After grain dilation optimization, the reconstructed grain size and grain boundary characters were calculated based on at least 800 grains. Pole figures were also constructed from the PED data for the texture analysis and compared to the XRD data.

Selected alloy thin films were also characterized by Atom Probe Tomography (APT) in a Cameca Scientific Instruments Local Electrode Atom Probe 3000XSi. The required needle shaped geometry was prepared in cross-section using a FIB lift out technique and an annular milling procedure described in reference [36] in either the TESCAN LYRA FIB- Field Emission Scanning Electron Microscope (SEM) or a FEI Quanta 3D dual beam FIB-SEM. The specimens were set at a base temperature 37 K where upon they were field evaporated with a laser energy of 0.3 nJ for a 0.5% targeted evaporation rate. The APT data was reconstructed using the IVAS 3.6.0 software platform.

3. Results

The in situ stress evolution of the 300 nm thick Fe, Cr and $Fe_{1-x}Cr_x$, where x ranged from 0.03 to 0.08, films are displayed in Fig. 1. Both Fe and Cr elemental thin films experienced post coalescence tensile stresses as similarly reported in the literature [16,27], with Cr being more tensile. As Cr was added to the Fe film, the tensile stress was lowered to be less than that of elemental Fe with a minimum stress for the $Fe_{0.96}Cr_{0.04}$ thin film.

Fig. 2 shows representative TEM bright field and PED plan view images for each of the films. The inset diffraction pattern was consistently indexed to a single BCC phase which was confirmed by the XRD scans. The PED scans from these films provide a clearer image of the grain sizes as well as revealing, in large part, that the grains are equiaxed. The PED scans also reveal a mosaic of colors that represent the different grain orientations; however, caution in interpreting texture should be used with these images and will be discussed further below. Fig. 3 (a–e) is the histograms of the grain sizes, which was calculated by the area fraction distribution, $F_A(D_i)$, given below

$$f_A(D_i)\delta D_i = \frac{A_i}{A_{total}} \quad (2)$$

where A_i is the area of grain 'i', A_{total} is the total area occupied by the grains which is equal to the surface of the measurement of all the pixels belonging to the grains [37], and δD_i is the bin size. Each histogram was fitted to a log normal function, superimposed in Fig. 3 [37,38], and showed good agreement for each composition, e.g. there was no noted abnormal grain growth. Fig. 3(f) is the cumulative grain size distribution plot from the mean grain sizes taken from the former histograms for the $Fe_{1-x}Cr_x$ (x = 0–0.08) thin films. The initial addition of Cr resulted in a shift in the distribution to a larger value up to 4 at.% Cr. Further increases in Cr resulted in refinement of the grain sizes towards the initial elemental Fe values.

Fig. 4 (a)–(c) is the pole figures generated from the PED and XRD scans. The high intensity region in the center of each scan denotes a strong ⟨110⟩ fiber texture. Though the PED images, Fig. 2, show some amount of variation in orientation color, the pole figure of Fig. 4(a) is a much more quantitative means of comparison. The pole figure provides the relative orientation of all the grains with respect to each other around a defined texture. The variation of orientation colors in Fig. 2 is attributed to the TEM foil being slightly titled relative to the beam normal during acquisition. To validate that the PED pole figures (as well as acquire a larger sampling of the film), XRD pole figures, Fig. 4(b)-(c), were captured. These confirmed the same ⟨110⟩ fiber texture. As the XRD scan acquired some residual intensities from the

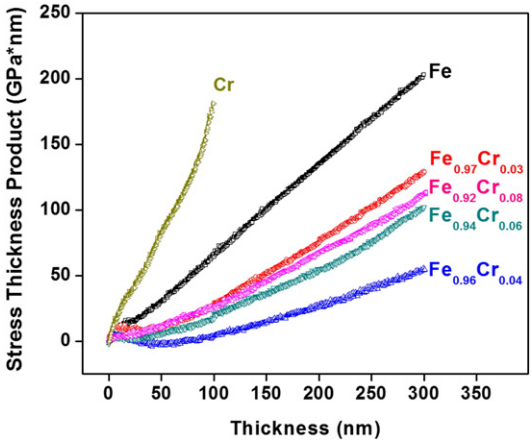

Fig. 1. Plot of stress thickness product versus thickness for films deposited at different Cr contents — $Fe_{1-x}Cr_x$, x = 0, 0.03, 0.04, 0.06, 0.08 and 1.00. Color available on-line.